NASA Technical Memorandum

NASA TM - 86569

ELECTRICAL PROPERTIES OF Al-In-Sn ALLOYS DIRECTIONALLY SOLIDIFIED IN HIGH AND LOW GRAVITATIONAL FIELDS

Center Director's Discretionary Fund Final Report

By P. A. Curreri, M. K. Wu, J. R. Ashburn, and W. K. Kaukler

Space Science Laboratory
Science and Engineering Directorate

October 1986

National Aeronautics and Space Administration

George C. Marshall Space Flight Center

TECHNICAL REPORT STANDARD TITLE PAGE

1. REPORT NO.	2. GOVERNMENT ACCESSION NO.	3. RECIPIENT'S CATALOG NO.
NASA TM-86569		

4. TITLE AND SUBTITLE	5. REPORT DATE
Electrical Properties of Al-In-Sn Alloys Directionally Solidified in High and Low Gravitational Fields — Center Director's Discretionary Fund Final Report	October 1986
	6. PERFORMING ORGANIZATION CODE
7. AUTHOR(S) P. A. Curreri, M. K. Wu,* J. R. Ashburn,* and W. F. Kaukler**	8. PERFORMING ORGANIZATION REPORT #
9. PERFORMING ORGANIZATION NAME AND ADDRESS George C. Marshall Space Flight Center Marshall Space Flight Center, Alabama 35812	10. WORK UNIT NO.
	11. CONTRACT OR GRANT NO.
	13. TYPE OF REPORT & PERIOD COVERED Technical Memorandum
12. SPONSORING AGENCY NAME AND ADDRESS National Aeronautics and Space Administration Washington, D.C. 20546	14. SPONSORING AGENCY CODE

15. SUPPLEMENTARY NOTES

Prepared by Space Science Laboratory, Science and Engineering Directorate.
*Department of Physics, The University of Alabama in Huntsville.
**Department of Chemistry, The University of Alabama in Huntsville.

16. ABSTRACT

Al-In-Sn alloys have been directionally solidified in the NASA KC-135 aircraft which flies a series of parabolas to generate high (high-g) and low gravity (low-g) forces parallel to the longitudinal growth axis. Thus, for a given sample, successive sections can be identified which were solidified in high-g and low-g. Measurements of the electronic properties of the samples reveal that: (1) the resistivity of the low-g sections is larger (about a factor of 10) than that of the high-g sections; (2) the low-g sections behave conductively like a semi-metal, while the high-g sections are essentially metallic; and (3) both high-g and low-g sections are superconducting but the superconducting transition temperature of the low-g sections is 1 K higher than that of the high-g sections.

17. KEY WORDS	18. DISTRIBUTION STATEMENT
Alloy Directional Solidification, Low Gravity, Al-In-Sn, Immiscible Alloy Solidification, Electronic Properties	Unclassified — Unlimited

19. SECURITY CLASSIF. (of this report)	20. SECURITY CLASSIF. (of this page)	21. NO. OF PAGES	22. PRICE
Unclassified	Unclassified	20	NTIS

For sale by National Technical Information Service, Springfield, Virginia 22151

ACKNOWLEDGMENTS

The authors wish to thank M. H. McCay for her invaluable contribution to the solidification study and J. Coston for the WDX analysis and the SEM work. We would also like to thank G. Workman, G. Smith, and D. Warden for their careful preparation of the samples. This work was supported by the Marshall Space Flight Center Director's Discretionary Fund and the Research Institute of the University of Alabama in Huntsville.

TABLE OF CONTENTS

LIST OF ILLUSTRATIONS

TECHNICAL MEMORANDUM

ELECTRICAL PROPERTIES OF Al-In-Sn ALLOYS DIRECTIONALLY SOLIDIFIED IN HIGH AND LOW GRAVITATIONAL FIELDS

Center Director's Discretionary Fund Final Report

INTRODUCTION

The feasibility of producing high volume fraction immiscible alloys with finely dispersed microstructure by low-gravity solidification was demonstrated in 1974 [1]. Ga-Bi samples solidified in free fall, with a gravity level of 10^{-4} g (g = 980 cm/s^2), had much finer microstructure than the control samples solidified in normal gravity. It was also found that the electrical properties of the low-gravity solidified materials were significantly different from those of the control samples solidified under the same conditions except at one gravity [2]. The potential to synthesize in space a new class of electronic materials was suggested by these initial experiments. However, extensive studies along this line in space are limited due to high cost and limited access to orbital experimentation facilities.

In an attempt to gain more insight into the low-gravity processing on the material properties of immiscible alloys, we decided to carry out a systematic study of materials solidified directionally in a Bridgman furnace on NASA's KC-135 aircraft. The advantages of using KC-135 are that it is relatively inexpensive, has a short turnaround time, and provides the capability when combined with unidirectional solidification of having in one sample a series of identifiable sections grown in low-g or high-g [3-5]. The material chosen in this study is the ternary Al-In-Sn alloy [6]. This alloy was chosen because the Al-In binary has been well studied and the addition of Sn to the Al-In binary would alter the interphase interfacial energy and the morphology of the solid-liquid interface and therefore the cast structure. This study would then help to identify the role of interphase interfacial energies during solidification with varying g levels. In addition, the electrical properties of the binary Al-In, Al-Sn, and In-Sn alloys have been extensively studied. Therefore, an extension of the study to the ternary system is a logical choice. The specific material studied in this report is the Al-18.9In-14.6Sn in weight percent.

EXPERIMENTALS

The Al-In-Sn alloys were directionally solidified in a high temperature Bridgman-type furnace with a water-cooled quench block. The furnace system was used to process samples during maneuvers of NASA's KC-135 aircraft. The aircraft flies a series of parabolas during which the onboard experiment experiences up to 30 s of low gravity and up to 1.5 min of pullout and climb with up to 1.7 g acceleration. Therefore, a sample which is being solidified experiences a repetitive sequence of low-g and high-g forces parallel to the longitudinal growth axis. The acceleration during processing is monitored by three accelerometers mounted on the furnace on orthogonal axes with one parallel to the longitudinal growth axis. For a typical maneuver during low-g, the acceleration on all axes averages below 10^{-2} g [7]. During pullout and climb, the high-g acceleration parallel to the sample longitudinal

axis reaches 1.7 g while the acceleration on the other axes is less than 0.15 g. The growth rate for the Al-18In-14Sn sample was 0.5 cm per minute. This results in low-g sections of about 2.5 mm alternating with high-g sections of about 7.5 mm. The samples were positioned relative to the thermal gradient of the furnace to allow about 2 cm of the sample to remain unmolten prior to directional solidification.

The solidified sample (8 cm long x 5 mm dia.) was first cut and mounted longitudinally, then polished using successively smaller grit. The metallographically polished sample was examined under an optical microscope in reflected light to determine the location of the boundary where directional solidification was initiated. Growth rate and accelerometer data were then used to correlate position on the sample with gravitational acceleration during solidification. A photomicrograph of Al-18.9In-14.6Sn flight sample for which properties data are reported here is shown in Figure 1. Samples of different gravity level were sectioned using a diamond saw, and smaller samples of dimension 1 mm x 1 mm x 3 mm were cut and used for electrical and magnetic properties measurements. The conventional d.c. or a.c. four-probe method was used for the electrical resistivity measurements. An a.c. inductance bridge operated at 40 Hz was used to measure the magnetic susceptibility. Transverse sections of different gravity level were mounted and polished for scanning electron microscope (SEM) study. Wavelength dispersive x-ray (WDX) analysis was employed to determine the chemical composition of the samples.

RESULTS

Typical resistance, R, of samples solidified at different gravity levels is shown in Figure 2 as a function of temperature. It can be seen that the resistance of low-g samples is less temperature-dependent. Table 1 summarizes the electrical properties of the samples measured which includes the sample section prior to directional solidification and In-Sn alloys of two selected compositions. The resistance ratio [defined as $R(300\ K)/R(T_c)$ where T_c is the onset temperature of the superconducting transition] of high-g samples is larger than that of low-g samples. On the other hand, the room temperature resistivity of the low-g samples is about a factor of 10 larger than that of the high-g samples. Figure 3 is a schematic plot showing resistance as a function of temperature for typical semi-metal and metal with a superconducting transition at low temperature. Results given in Figure 2 in comparison to the characteristic curves in Figure 3 clearly indicate that the low-g sample behaves more like a semi-metal while the high-g sample is essentially metallic.

All samples studied become superconducting with an onset temperature ranging from 7.8 K to 6.3 K. Figure 4 shows the temperature dependence of the resistance and magnetic susceptibility at low temperature for a high- and low-g sections. The average transition width is 3 K, showing the inhomogeneous character of our material. Since our main interest lies in the comparison of the characteristics of the low-g and high-g samples, we have taken the onset temperature of the transition as T_c. T_c, resistance ratio, and the gravitational acceleration parallel to the growth axis during solidification as plotted versus sample position are shown in Figure 5.

In Figure 6, we have shown an example of the detailed resistive behavior of a sample (Section 7) at low temperature. An unusual electrical anomaly is observed for both low-g and high-g samples in the temperature regime right before the complete superconducting transition. The resistance first decreases on cooling and then suddenly rises before the complete transition. The magnitude of the anomaly depends on the measuring currents. A measuring current larger than 10 mA is found to

completely suppress the anomaly, leaving only the lower temperature superconducting transition (where T_c is defined). An external magnetic field of 300 G is also found to suppress the observed anomaly. It should be noted that such an anomaly is not characteristic of an inhomogeneous sample with broad superconducting transition. In addition, such an anomaly was not observed in the ground processed In-Sn samples.

Microstructure and chemical composition analyses of the samples have been performed using a SEM fitted with a WDX analyzer. The micrographs clearly show that the samples consist of particles of 10 to 50 μm in size embedded in the aluminum matrix. It is found that there are two different phases in these particles, viewed as dark and light particles in the light field SEM. The apparent volume fraction of the dark phase is about one-third of the particles. These particles are made almost entirely of In and Sn. The dark phase of the particles consists of In-Sn with 25 wt.% Sn and the Sn content does not change with g-level during solidification. On the other hand, the Sn concentration of the light phase of the particles does appear to vary with gravity level. The low-g light particle is mainly In-Sn with 25 wt.% Sn, while its counterpart in high-g is mainly In-Sn with 75 wt.% Sn. A summary of the results is also given in Table 1. WDX measurements at 200X magnification show little variation in overall composition as function of gravity level.

DISCUSSION

The results given in Table 1 and Figure 5 clearly demonstrate that the accelerations during solidification greatly affect the electrical properties of the sample. The electrical behavior evidenced by small overall resistance ratio indicates that the samples studied are indeed inhomogeneous or polyphase. Their resistivities are dominated by the scattering of electrons by the dispersion of second phase which is the precipitated In-Sn embedded in the aluminum matrix if we consider the connecting path of the electron is the aluminum matrix. It is known that the electrical properties of an alloy depend on its particle size and the interface between particles [8]. Smaller particles will lead to an increase in the surface-to-volume ratio with a subsequent increase in electron scattering and interface effects. The relatively smaller resistance ratio and the larger room temperature resistivity of the low-g sample over those of the high-g samples suggest that samples solidified at low-g may consist of finely dispersed particles. Unfortunately, we do not see any clear difference in particle size between low-g and high-g samples from photomicrographs. This suggests that the conducting path may be different for samples solidified at different gravity level.

Based on the WDX composition analysis, it can be inferred from the phase diagram that low-g samples contain mainly β phase (25 wt.% Sn) In-Sn particles, while the high-g samples consist of small portions of β phase particles randomly distributed in the larger γ phase (75 wt.% Sn) particles. Therefore, it is not unreasonable to assume that for the high-g samples, the connectivity of the conducting path is through the aluminum matrix, and for the low-g samples, it is through the precipitated In-Sn particles. This model is shown schematically in Figure 7. The observation of the resistive behavior of the ground processed In-Sn samples, which is similar to that of the low-g samples but different from that of the high-g samples, seems to support such an assumption. With this model, the scattering centers are then the smaller dark particles and the larger light particles for the low-g and high-g samples, respectively. As mentioned earlier, the size of the dark particles is about one-third that of the light particles. This corresponds to a factor of 10 reduction

in surface-to-volume [8] ratio for the dark particles. A factor of 10 increase in resistivity in low-g samples is then expected. This is consistent with the observed difference in room temperature resistivity and resistance ratio between the low-g and high-g samples. A photomicrograph study of the deep etched sample indeed shows that the precipitated particles are more dense in the low-g sections than in the high-g sections, but attempts to quantitatively verify the difference in the connectivity of the In-Sn phase have been thus far inconclusive.

The superconductivity observed is attributed to the presence of the In-Sn phase. Superconductivity of the In-Sn system has been extensively studied [9-11]. It was found that T_c of the quenched samples varies from 7.8 K to 5.5 K with Sn content [9]. Peak T_c of 7.8 K occurs at the β phase with composition of 30 wt.% Sn, while γ phase alloys have T_c on the order of 6 K. Superconducting transition temperature of In-Sn alloys as a function of Sn content along with the In-Sn binary phase diagram is shown in Figure 8. This is consistent with our observations that low-g samples have T_c about one degree higher than that of the high-g samples, and our hypothesis based on WDX analysis that the low-g particles are essentially β phase while high-g sections contain mainly γ phase particles.

The resistive anomaly observed at low temperature is rather unusual. The dependence of the anomaly on transport currents and external magnetic fields indicates that the anomaly is superconducting in origin. It suggests that the sample undergoes a normal → superconducting → normal → superconducting transition. It is known that a granular superconductor, in which the superconducting grains are coated with an insulating layer or imbedded in an insulating matrix, may exhibit reentrant superconductivity [12-14]. In view of the inhomogeneous nature of our sample, it is very possible that there exist small superconducting grains coated with thin insulating film that have relatively larger T_c than that of the major In-Sn particles. The observed resistive behavior can then be understood as follows: as temperature decreases, superconductivity appears in the small grains and phase matching between grains is established through Josephson coupling, resulting in the decrease in resistance. Upon further cooling, decoupling between the superconducting grains occurs when the resistance of the insulating film reaches a certain value and results in an increase in resistance. However, at a lower temperature where the major In-Sn particles become superconducting, a complete transition occurs through the connectivity of these particles. The facts that a magnetic field of 300 G and a current density of 1 A/cm^2 completely suppressed the anomaly indicate that the superconductivity of these small grains is a weak coupling type. At this moment, whether the exact origin of this superconductivity is due to the In-Sn micrograins or some unidentified phases (such as interfacial effects [15] between particles) is unknown. The absence of the anomaly in the ground processed In-Sn samples suggests that the presence of aluminum may play an important role. It should be noted that such a "tricriticle transition" has been observed in an Au/Ge alternating ultra-thin layered film [16].

The observation of a preferential phase formation at different gravity of the Al-In-Sn system is surprising. More detailed compositional study of the samples is being pursued. A careful analysis of the microstructure in relation to the phase diagram is underway. The results will be presented in a separate paper.

In conclusion, we have studied the ternary, Al-18.9In-14.6Sn directionally solidified in NASA KC-135 aircraft. Electrical properties measurements of the samples solidified at different g levels show that: (1) Low-g samples behave more like a

semi-metal while high-g samples are essentially metallic. (2) Both low-g and high-g samples are superconducting but T_c of low-g samples is 1 K higher than that of high-g samples. (3) A resistive anomaly attributed to reentrant superconductivity is observed in the samples studied.

REFERENCES

1. Reger, J. L. and Yates, I. C., Jr.: AIAA Paper No. 74-207, Washington, D. C., 1974.

2. Lacy, L. L. and Otto, G. H.: AIAA Paper No. 74-208, Washington, D. C., 1974.

3. Johnston, M. H., Curreri, P. A., Parr, R. A., and Alter, W. S.: Metall. Trans., Vol. 16A, 1985, p. 1683.

4. Stefanescu, D. M., Curreri, P. A., and Fiske, M. R.: Metall. Trans., Vol. 17A, 1986, p. 1121.

5. Lee, J. E., McCay, M. H., and Curreri, P. A.: Metall. Trans., A, in press, 1986.

6. (a) Campbell, A. N., Buchanan, L. B., Kuzmak, J. M., and Tuxworth, R. H.: J. Am. Chem. Soc., Vol. 74, 1952, p. 1952. (b) Grugel, R. N. and Hellawell, A.: Metall. Trans., Vol. 12A, 1981, p. 669. (c) Derby, B., Camel, D., and Favier, J. J.: J. Crystal Growth, Vol. 65, 1983, p. 280.

7. Hendrix, J. C., Curreri, P. A., and Stefanescu, D. M.: AFS Trans., Vol. 92, 1984, p. 435.

8. Maeden, G. T.: Electrical Resistance of Metals, Plenum Press, New York, 1965.

9. Wernick, J. H. and Matthias, B. T.: J. Chem. Phys., Vol. 34, 1961, p. 2194.

10. Merriamm, M. F. and Von Herzen, M.: Phys. Rev., Vol. 131, 1963, p. 637.

11. Bartram, S. F., Moffatt, W. G., and Roberts, B. W.: J. Less-Common Metals, Vol. 62, 1978, p. 9.

12. Abeles, B.: Phys. Rev., Vol. B15, 1977, p. 2828.

13. Ambegaokar, V. and Baratoff, A.: Phys. Rev. Lett., Vol. 10, 1963, p. 486.

14. Itskovish, I. F. and Shekhter, R. I.: Fiz. Nizk. Temp., Vol. 7, 1981, p. 863. [Sov. J. Low Temp. Phys., Vol. 7, 1981, p. 418].

15. Geballe, T. H. and Chu, C. W.: Comm. Solid State Phys., Vol. 9, 1979, p. 115.

16. Akihama, R. and Okamoto, Y.: Solid State Commun., Vol. 53, 1985, p. 655.

TABLE 1. ELECTRICAL PROPERTIES OF Al-18.9In-14.6Sn

Sample No.	ρ(273 K) ($\mu\Omega$-cm)	ρ(273 K)/$\rho(T_c)$	T_c (K)	Sn Content (wt.%) (LPP)	(DPP)	G
1	13.5	38.3	6.5	24	19	1
2	121.2	1.54	7.4	26	25	Low
3-1	9.3	25.4	6.7	72	19	High
3-2	103.2	7.9	7.1	22	19	Low
4	19.1	15.2	6.5	68	21	High
5	123.6	5.6	7.8	26	19	Low
6	14.9	4.7	6.7	50	21	High
7-1	731.7	0.78	7.3	21	26	Low
7-2	395.2	1.8	7.4	21	26	Low
8	15.5	13.9	6.5	73	26	High
9	46.7	2.4	7.3	-	-	Low
Al	1.17	4.2×10^3	1.17			
$In_{75}Sn_{25}$ (β)	56.1	2.15	7.1			
$In_{25}Sn_{75}$ (γ)	70.1	2.57	6.4			

LPP: Light Phase Particles
DPP: Dark Phase Particles
G: Level of Acceleration

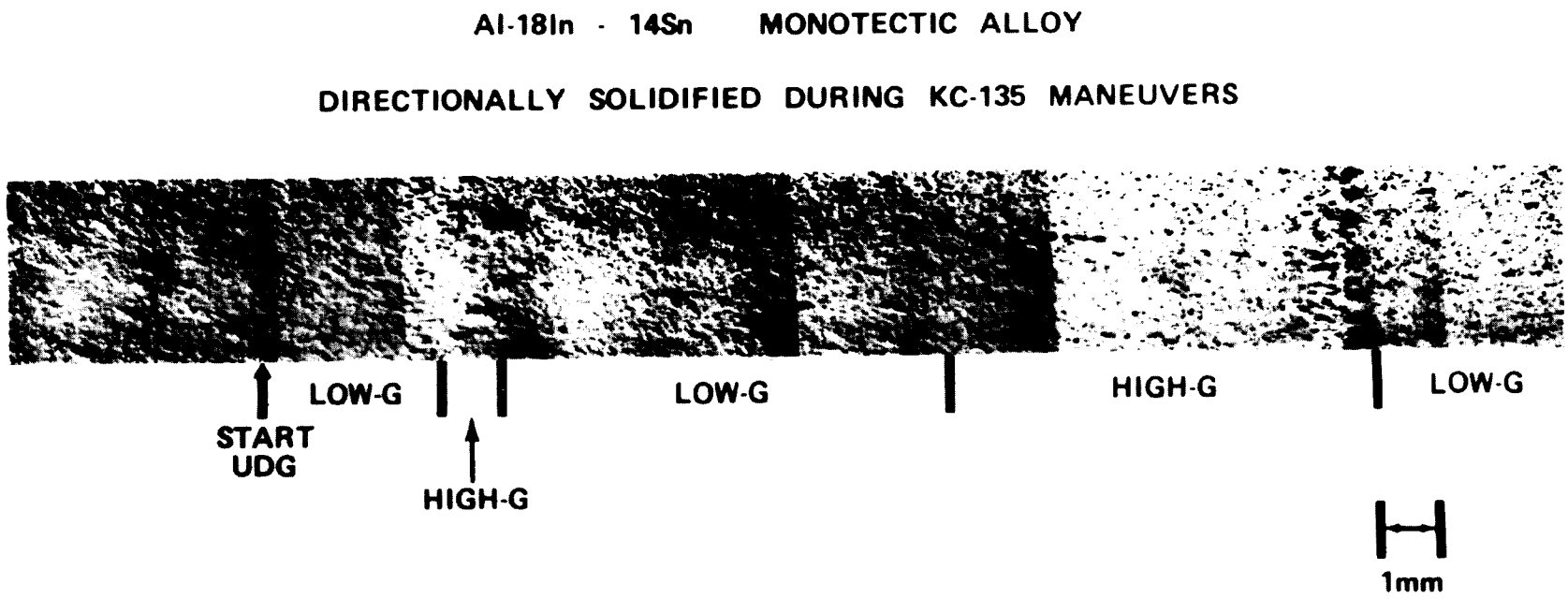

Figure 1. Photomicrograph of Al-18.9In-14.6Sn along the longitudinal growth axis showing the microstructure of the sample up to the third low-g zone.

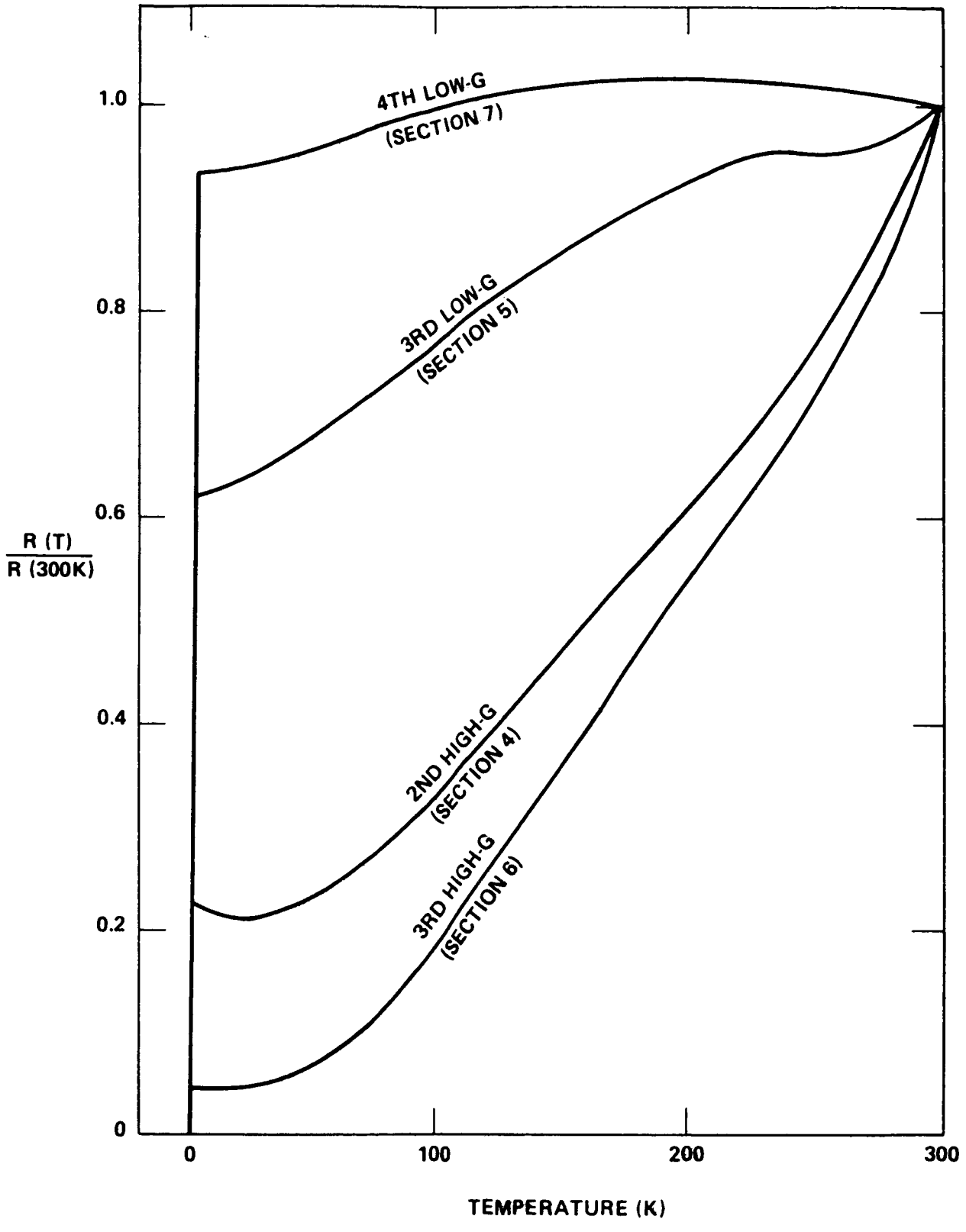

Figure 2. Normalized resistance $R(T_c)/R(300\ K)$ as a function of temperature of Al-18.9In-14.6Sn sections solidified under different levels of acceleration.

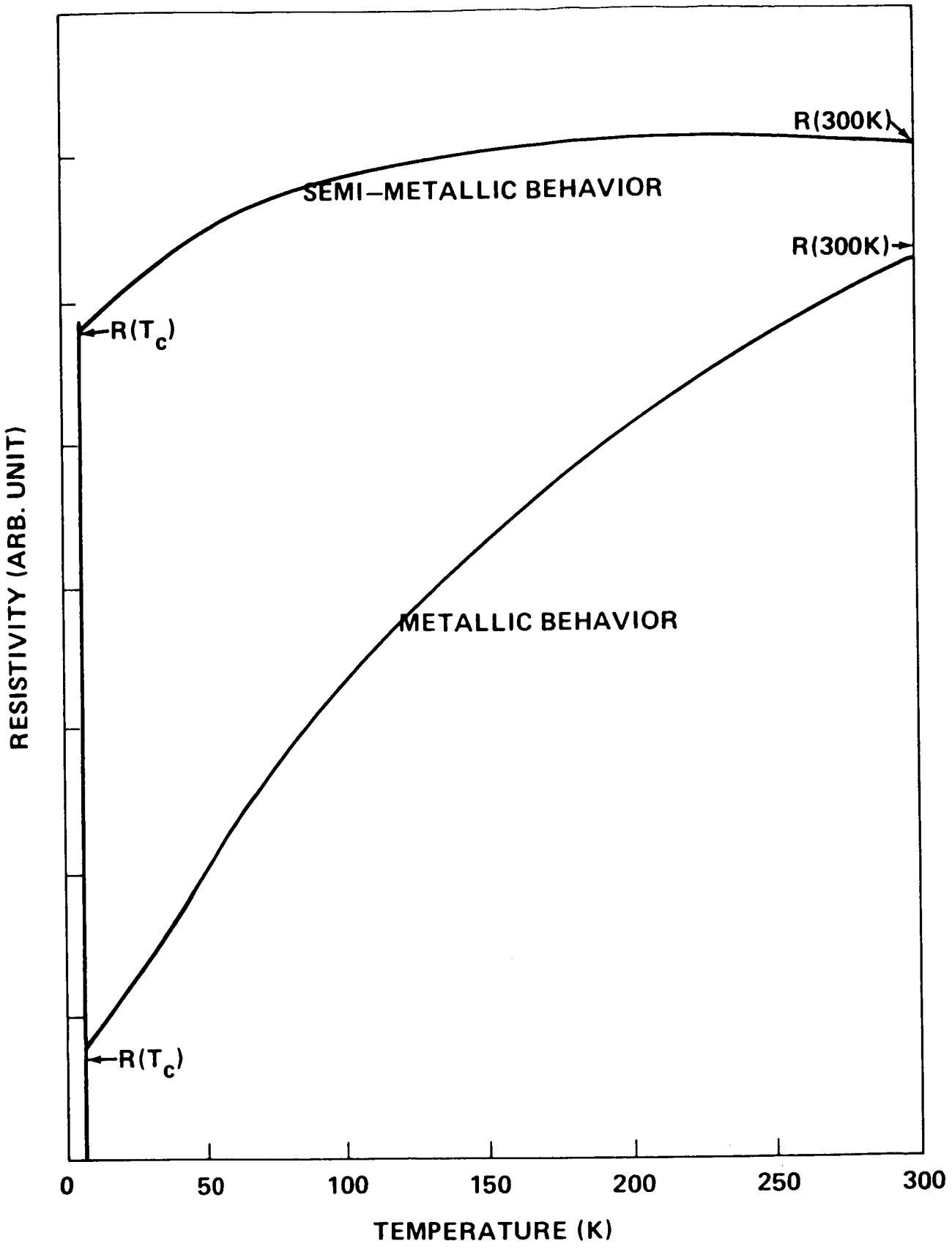

Figure 3. Schematic plot illustrating the characteristic behavior of resistance as a function of temperature for semi-metal and for metal with superconducting transition at low temperature.

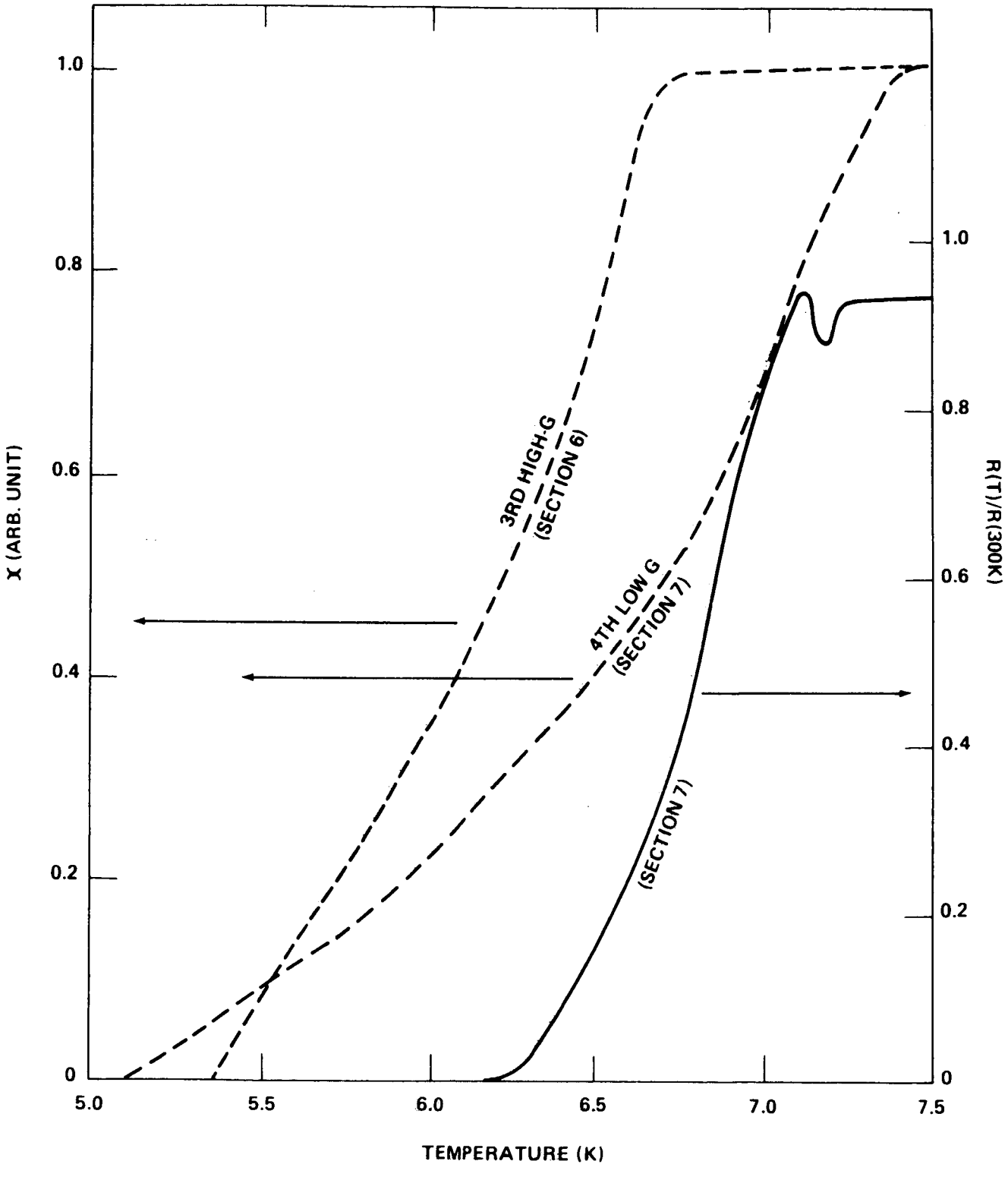

Figure 4. Electrical resistance and magnetic susceptibility at low temperature of Al-18.9In-14.6Sn solidified under different levels of acceleration.

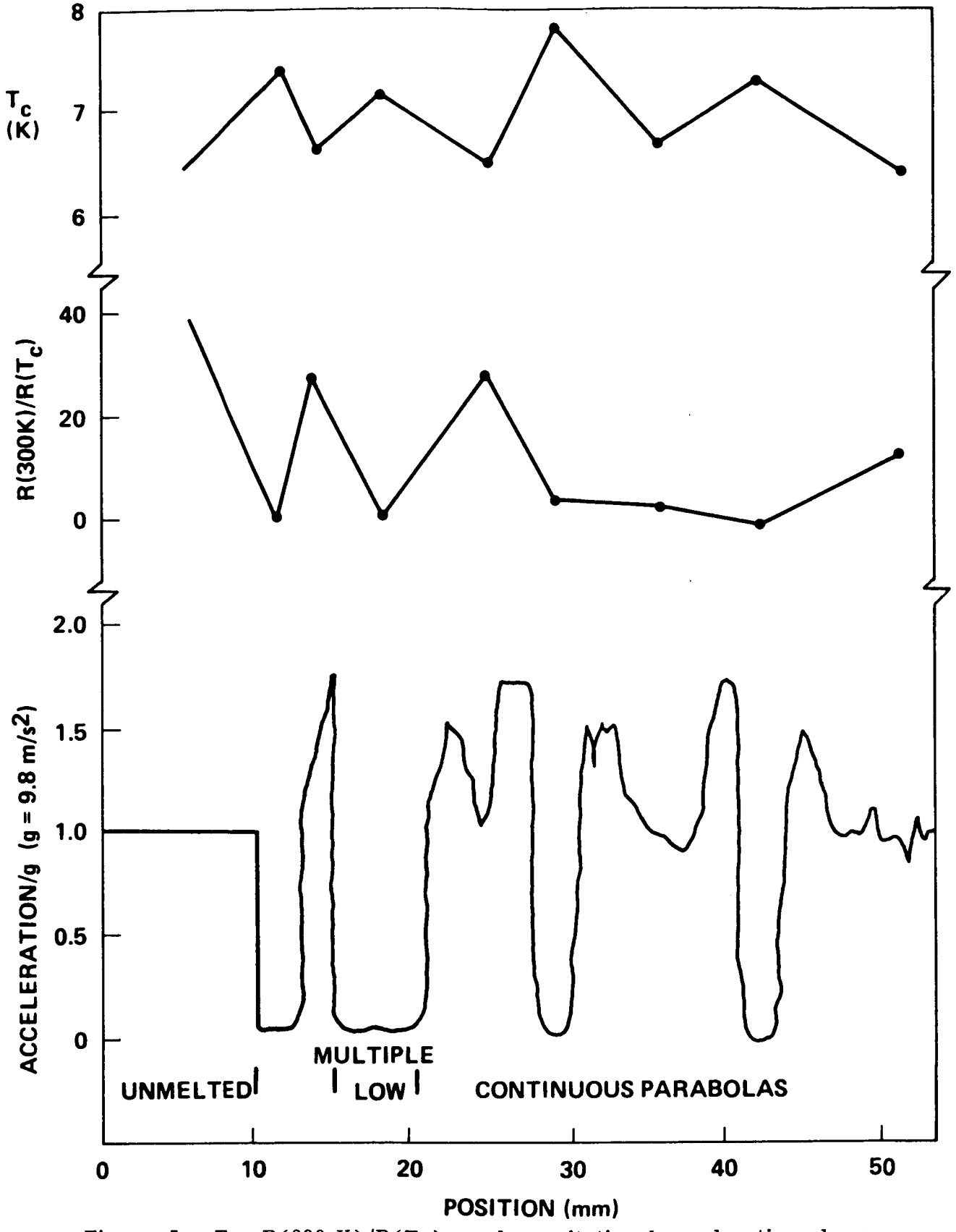

Figure 5. T_c, R(300 K)/R(T_c), and gravitational acceleration along the longitudinal growth axis as a function of sample position.

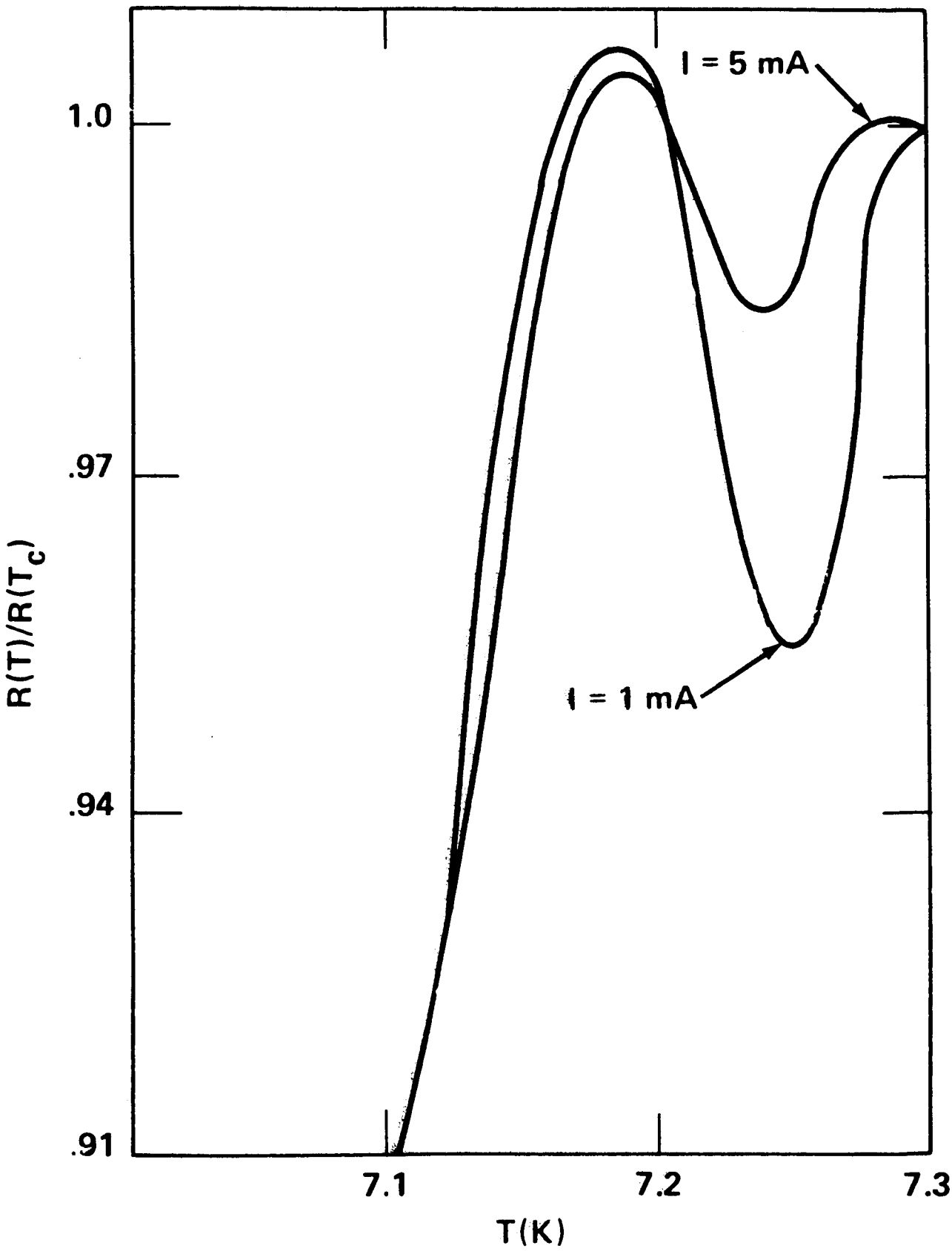

Figure 6. Detail of the electrical resistance as a function of temperature near the superconducting transition temperature, T_c, at two measuring currents.

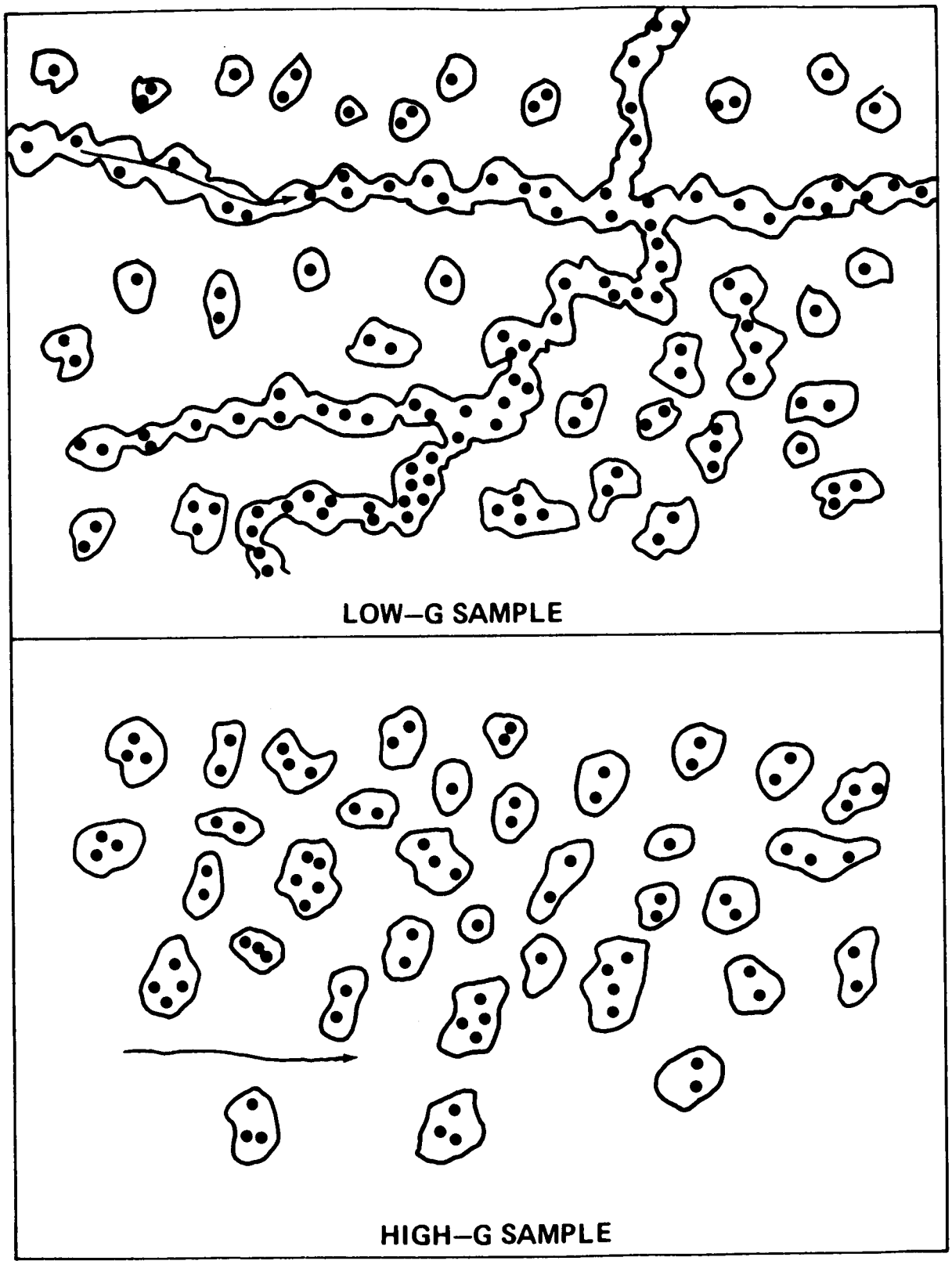

Figure 7. Schematic plot showing the proposed model for the current conducting path for sample solidified in low g and in high g.

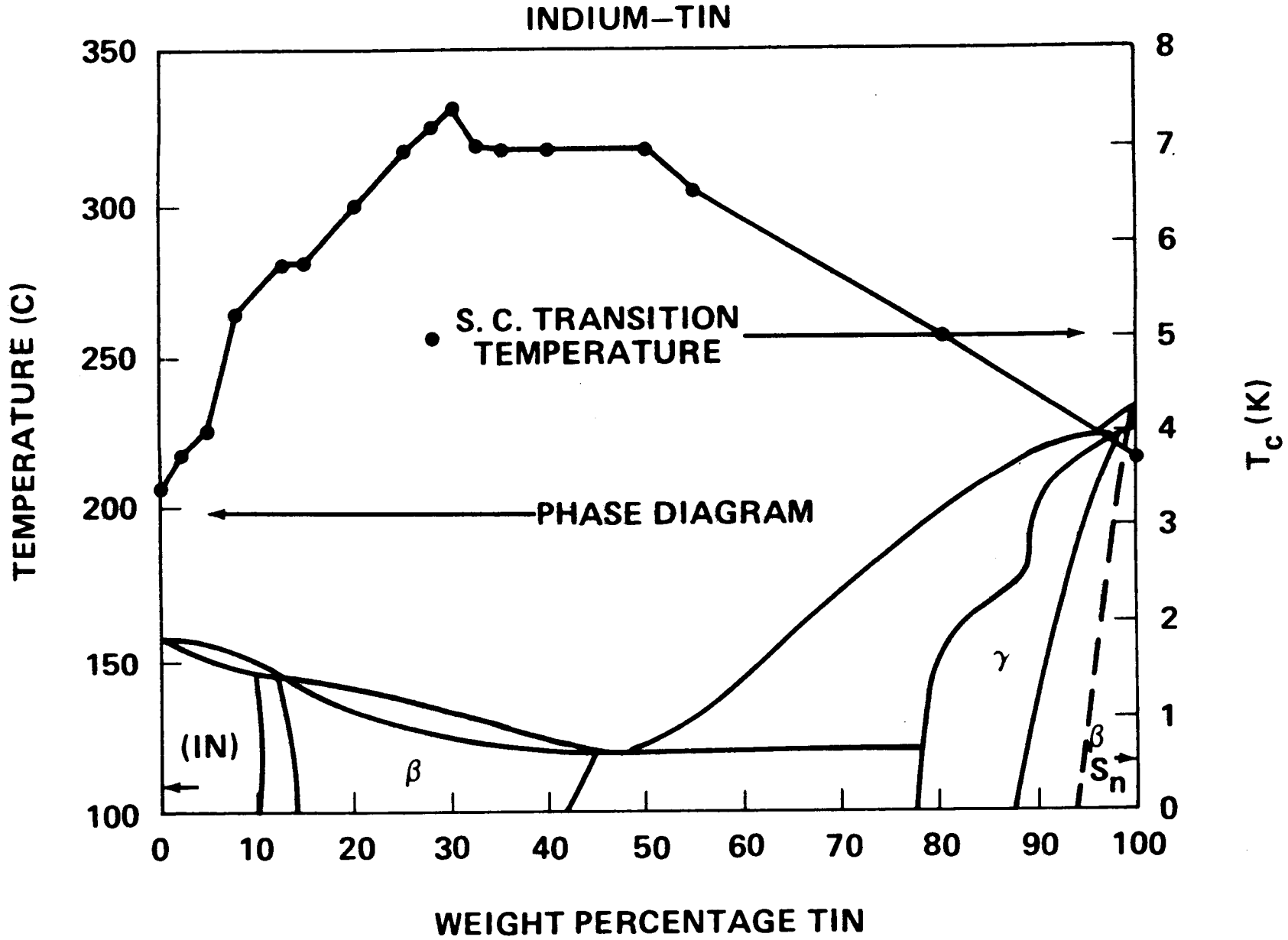

Figure 8. Superconducting transition temperature plotted versus Sn concentration and the phase diagram of In-Sn alloys (T_c data taken from Reference 9).

APPROVAL

ELECTRICAL PROPERTIES OF Al-In-Sn ALLOYS DIRECTIONALLY SOLIDIFIED IN HIGH AND LOW GRAVITATIONAL FIELDS

Center Director's Discretionary Fund Final Report

By P. A. Curreri, M. K. Wu, J. R. Ashburn, and W. F. Kaukler

The information in this report has been reviewed for technical content. Review of any information concerning Department of Defense or nuclear energy activities or programs has been made by the MSFC Security Classification Officer. This report, in its entirety, has been determined to be unclassified.

E. A. Tandberg-Hanssen

E. A. TANDBERG-HANSSEN
Deputy Director, Space Science Laboratory

☆U.S. GOVERNMENT PRINTING OFFICE 1986—730-067/40033